Solid State Phenomena
ISSN: 1662-9779, Vol. 388, pp 1-9
doi:10.4028/p-Maph4K

Submitted: 2025-12-05
Revised: 2026-02-18
Accepted: 2026-02-18
Online: 2026-04-15

Thickness Scaling of Forming Limit Curves

Holger Aretz

Speira GmbH, Research & Development, Georg-von-Boeselager-Str. 21, 53117 Bonn, Germany

holger.aretz@speira.com

Keywords: forming limit curve, FLC, Nakajima, thickness dependence, bending.

Abstract. A consistent kinematic method was developed to calculate a forming limit curve (FLC) for a material with thickness t_0^* from a given FLC pertaining to a different thickness $t_0 \neq t_0^*$. The developed method is based on the analysis of the bending strains introduced by the Nakajima test method. To calculate the required strains, an explicit and an implicit procedure are presented. In contrast to its implicit equivalent, the explicit method suffers from an intrinsic error which scales with the material's gauge and can be quantified by considering the neutral case $t_0^* = t_0$. Finally, the developed method predicts a linear relationship between $\mathrm{FLC}_{\mathrm{min}}$ and the material thickness, which is in line with practical experience.

Introduction

If rolled materials of the same grade are manufactured equivalently (e.g. identical relative rolling reductions and heat treatments), then many final properties (e.g. yield strength, tensile strength, uniform strain, r-values, etc.) are practically independent of their final gauge. However, all fracture-related characteristics display a significant thickness dependence. For example, the work of Suh *et al.* [6] suggests that the fracture strain in uniaxial tensile tests positively correlates with the sample gauge, which, in turn, directly determines the number of grains across thickness. A strong thickness dependence is also observed in forming limit curves (FLCs) acquired by the Nakajima stretch forming test. In this test, differently shaped sheet samples are stretched over a hemispherical punch until fracture. This introduces bending strains (e.g. Noder & Butcher [5]), which inevitably bias the failure strains measured at the surface. Consequently, for equivalent materials made of different gauges failure strains increase with thickness.

In the development phase of technical products, frequent design changes are very common and affect both the selection of suitable material grades and their gauge. A problem for sheet manufacturers is the fact that material data cannot be provided for any imaginable material grade and gauge. In particular, the lack of FLCs pertaining to the considered gauge is often problematic. Although some forming simulation codes provide a thickness adjustment feature for FLCs, the underlying approaches known to the author are based on empirical relationships (e.g. Abspoel *et al.* [1] and Banabic *et al.* [4, pp. 325-326]), which is not satisfactory.

In the present work, a consistent kinematic method was developed to calculate the FLC for a sheet material with thickness t_0^* from a given FLC pertaining to a different thickness $t_0 \neq t_0^*$. The developed method is based on the analysis of the bending strains introduced by the Nakajima test method. It is emphasized that the proposed kinematic method is unable to account for microstructural effects, such as those observed by Suh *et al.* [6].

Bending Strain Theory

In the following, the strain theory for shell bending derived in Timoshenko & Gere [7, pp. 440-441] is used to calculate in-plane strains in a bent shell. Note that the bending theory is formulated in terms of *engineering* strains. In general, principal components of the *engineering* strain tensor are denoted by e_j, whereas ε_j is used for *logarithmic* principal strains. If needed, logarithmic strains can be converted to engineering strains according to $e_j = \exp(\varepsilon_j) - 1$ and vice versa. The notational

convention $\varepsilon_1 \geq \varepsilon_2$ is used throughout this paper, i.e. ε_1 is the major principal strain and ε_2 the minor principal strain.

To ease navigation through the text, the following three geometric planes are defined:

(1) *Top surface plane:* in the Nakajima test, this is the *convex* side of the deformed sample. The associated engineering strain components are denoted as $e_{j,\mathrm{top}}$.

(2) *Bottom surface plane:* in the Nakajima test, this is the *concave* side of the deformed sample, which is in contact with the punch. The associated engineering strain components are denoted as $e_{j,\mathrm{bot}}$.

(3) *Midplane:* this is the plane halfway between the top and bottom surface. The associated engineering strain components are denoted as $e_{j,\mathrm{mid}}$.

According to Timoshenko & Gere [7, pp. 440-441], the *engineering* in-plane strains of a bent shell can be calculated from

$$e_j(z) = \frac{e_{j,\mathrm{mid}}}{1-\frac{z}{R_j}} - \frac{z}{1-\frac{z}{R_j}} \cdot \left[\frac{1}{(1-e_{j,\mathrm{mid}})\cdot\hat{R}_j} - \frac{1}{R_j}\right], \quad j = 1,2 \tag{1}$$

with R_j and $\hat{R}_j$ denoting the radius of curvature in the undeformed and deformed configuration, respectively (see also Axelrad [3, p. 32]). Note the singular cases $e_{j,\mathrm{mid}} = 1$ and $z/R_j = 1$. The coordinate $z \in [-t/2\,, t/2]$, with t being the shell's thickness, points towards the center point of curvature and is zero in the shell's midplane. Accordingly, at the *convex* side of the shell $z = -t/2$ and at the *concave* side $z = +t/2$. In the *undeformed* configuration the blank is *flat*, i.e. $R_j \to \infty$. Accordingly, Eq. (1) simplifies to

$$\underset{R_j\to\infty}{e_j(z)} = e_{j,\mathrm{mid}} - \frac{z}{(1-e_{j,\mathrm{mid}})\cdot\hat{R}_j}, \quad j = 1,2 \tag{2}$$

In the Nakajima test a hemispherical punch of radius R_p is used, along with a covering lubrication system of thickness t_lub. Thus, we may define an *effective* punch radius $R_\mathrm{p,eff}$ as follows:

$$R_\mathrm{p,eff} \coloneqq R_\mathrm{p} + t_\mathrm{lub} \tag{3}$$

The radius of curvature is then given by

$$\hat{R}_j = R_\mathrm{p,eff} + t/2\,, \quad j = 1,2 \tag{4}$$

with t being the current sample thickness. Even a rather large value of $t_\mathrm{lub} = 3$ mm causes a *relative* change of the strain results of only < 1 %. Thus, t_lub will be neglected, yielding the convenient approximation

$$\hat{R}_j \approx R_\mathrm{p} + t/2\,, \quad j = 1,2 \tag{5}$$

A very useful result can be derived from Eq. (1) by solving for $\hat{R}_j$, which yields

$$\hat{R}_j = \frac{z}{(1-e_{j,\mathrm{mid}})\cdot\left(e_{j,\mathrm{mid}} - e_j(z)\right)}, \quad j = 1,2 \tag{6}$$

However, $\hat{R}_j$ is the same for all $z \in [-t/2\,, t/2]$. Thus, for two positions z_1 and z_2 we obtain

$$\hat{R}_j = \frac{z_1}{(1-e_{j,\mathrm{mid}})\cdot\left(e_{j,\mathrm{mid}} - e_j(z_1)\right)} = \frac{z_2}{(1-e_{j,\mathrm{mid}})\cdot\left(e_{j,\mathrm{mid}} - e_j(z_2)\right)}, \quad j = 1,2 \tag{7}$$

Solving for $e_{j,\mathrm{mid}}$ finally yields

$$e_{j,\mathrm{mid}} = \frac{z_1\cdot e_j(z_2) - z_2\cdot e_j(z_1)}{z_1 - z_2}, \quad z_1 \neq z_2, \quad j = 1,2 \tag{8}$$

Note the similarity with the well-known *regula falsi* method to calculate roots of equations. Equation (8) reveals that the midplane strains can be calculated in terms of two known strains evaluated at arbitrary, but different, positions z_1 and z_2.

Another result that will be very useful is obtained by calculating the *average* in-plane strains, $e_{j,\mathrm{avg}}$, from Eq. (2) by means of the mean-value theorem:

$$e_{j,\mathrm{avg}} = \frac{1}{t} \cdot \int_{-\frac{t}{2}}^{+\frac{t}{2}} \left(e_{j,\mathrm{mid}} - \frac{z}{(1-e_{j,\mathrm{mid}}) \cdot \hat{R}_j} \right) \mathrm{d}z = e_{j,\mathrm{mid}}, \quad j = 1,2 \tag{9}$$

As one may see, the average in-plane strains are identical to the midplane strains.

From Eq. (2) we may deduce

$$e_{j,\mathrm{top}} \coloneqq e_j(z = -t/2) = e_{j,\mathrm{mid}} + \frac{t/2}{(1-e_{j,\mathrm{mid}}) \cdot \hat{R}_j}, \quad j = 1,2 \tag{10}$$

and

$$e_{j,\mathrm{bot}} \coloneqq e_j(z = t/2) = e_{j,\mathrm{mid}} - \frac{t/2}{(1-e_{j,\mathrm{mid}}) \cdot \hat{R}_j}, \quad j = 1,2 \tag{11}$$

The midplane strains $e_{j,\mathrm{mid}}$ can be calculated from Eq. (10) or Eq. (11) in terms of $e_{j,\mathrm{top}}$ and $e_{j,\mathrm{bot}}$, respectively. In either case, a quadratic equation is obtained which has only one physically plausible solution (cf. [2]):

$$e_{j,\mathrm{mid}} = \begin{cases} \frac{1+e_{j,\mathrm{top}}}{2} - \sqrt{\left(\frac{1+e_{j,\mathrm{top}}}{2}\right)^2 - \left(e_{j,\mathrm{top}} - \frac{t/2}{\hat{R}_j}\right)}, & j = 1,2 \\ \frac{1+e_{j,\mathrm{bot}}}{2} - \sqrt{\left(\frac{1+e_{j,\mathrm{bot}}}{2}\right)^2 - \left(e_{j,\mathrm{bot}} + \frac{t/2}{\hat{R}_j}\right)}, & j = 1,2 \end{cases} \tag{12}$$

Remarks:

(1) Equation (12) reveals a nonlinear dependence of the midplane strains $e_{j,\mathrm{mid}}$ on the current thickness t. Thus, the calculation of $e_{j,\mathrm{mid}}$ requires an iterative procedure, as discussed below.

(2) By re-arranging the arguments of the respective square roots, it may be seen that the first case of Eq. (12) produces always real solutions for $e_{j,\mathrm{mid}}$. In contrast, the second case may produce complex solutions if $(t/2)/\hat{R}_j$ becomes sufficiently large (indicating that shell bending theory is inapplicable) and/or if $e_{j,\mathrm{bot}} \to 1$. Thus, in computations it is advisable to check the sign of the square root's argument. □

For $(z_1, z_2) = (-t/2\,, t/2)$ Eq. (8) yields the following useful relationship:

$$e_{j,\mathrm{mid}} = \frac{e_{j,\mathrm{top}} + e_{j,\mathrm{bot}}}{2}, \quad j = 1,2 \tag{13}$$

Thus, when $e_{j,\mathrm{mid}}$ is known by Eq. (12) in terms of $e_{j,\mathrm{top}}$, Eq. (13) can be used to calculate $e_{j,\mathrm{bot}}$ and vice versa. Equation (13) may also be obtained by adding Eq. (10) and Eq. (11).

Remarks:

(1) For the special case $e_{j,\mathrm{top}} = -e_{j,\mathrm{bot}}$ Eq. (13) yields $e_{j,\mathrm{mid}} = 0$, and vice versa.

(2) The relationship $e_{j,\mathrm{top}} = -e_{j,\mathrm{bot}}$ in terms of engineering strains does *not* imply $\varepsilon_{j,\mathrm{top}} = -\varepsilon_{j,\mathrm{bot}}$ in terms of logarithmic strains. This may be readily seen by converting the engineering strains to their logarithmic counterparts. □

Assuming volume constancy, we may calculate the *average thickness strain* in terms of the average in-plane strains $e_{1,\mathrm{avg}}$ and $e_{2,\mathrm{avg}}$ given by Eq. (9):

$$e_{3,\mathrm{avg}} = \frac{1}{(1+e_{1,\mathrm{avg}}) \cdot (1+e_{2,\mathrm{avg}})} - 1 = \frac{1}{(1+e_{1,\mathrm{mid}}) \cdot (1+e_{2,\mathrm{mid}})} - 1 \tag{14}$$

The current thickness is then

$$t = t_0 \cdot \left(1 + e_{3,\mathrm{avg}}\right) = \frac{t_0}{(1+e_{1,\mathrm{mid}}) \cdot (1+e_{2,\mathrm{mid}})} \tag{15}$$

Computational Procedure

For notational convenience, different FLCs are introduced. The *known* FLC pertaining to a sample thickness of t_0 is related to the *top* surface of the sample. Accordingly, the array holding the measured surface strain data (n strain couples) is denoted as $\mathbf{FLC}_{\mathrm{top}}$:

$$\mathbf{FLC}_{\mathrm{top}} = \begin{bmatrix} (\varepsilon_{1,\mathrm{top}}, \varepsilon_{2,\mathrm{top}})_1 \\ (\varepsilon_{1,\mathrm{top}}, \varepsilon_{2,\mathrm{top}})_2 \\ \vdots \\ (\varepsilon_{1,\mathrm{top}}, \varepsilon_{2,\mathrm{top}})_n \end{bmatrix} \tag{16}$$

Likewise, the arrays holding the FLC data referred to the *bottom* surface and the *midplane* will be denoted as $\mathbf{FLC}_{\mathrm{bot}}$ and $\mathbf{FLC}_{\mathrm{mid}}$, respectively. The FLCs pertaining to another sample thickness $t_0^* \neq t_0$ are denoted as $\mathbf{FLC}^*_{\mathrm{top}}$, $\mathbf{FLC}^*_{\mathrm{bot}}$ and $\mathbf{FLC}^*_{\mathrm{mid}}$, respectively.

The overall objective is to calculate $\mathbf{FLC}^*_{\mathrm{top}}$ from $\mathbf{FLC}_{\mathrm{top}}$. The developed computational procedure may be broken down in two major steps: in the first step, the top surface strains of the given forming limit curve are used to calculate the corresponding bottom surface strains; in the second step, the calculated bottom surface strains are used to calculate the top surface strains using the desired new material thickness. The following assumptions are introduced:

Assumption 1. The deformation is isochoric (volume preserving).

Assumption 2. The failure strains at both bottom surfaces are identical:

$$\mathbf{FLC}^*_{\mathrm{bot}} = \mathbf{FLC}_{\mathrm{bot}} \tag{17}$$

Assumption 3. The strain ratios at both top surfaces are identical:

$$\frac{(\varepsilon_{2,\mathrm{top}})_k}{(\varepsilon_{1,\mathrm{top}})_k} = \frac{(\varepsilon^*_{2,\mathrm{top}})_k}{(\varepsilon^*_{1,\mathrm{top}})_k} \tag{18}$$

for each FLC point $k \in [1, n]$, with $n \in \mathbb{N}^*$ being the total number of FLC points.

In detail, the computational procedure consists of more than two steps. The bending strain theory formulated above is used to perform the required calculations. In the following, two algorithms will be formulated which differ in the way the current thicknesses t and t^*, respectively, are computed; the utilized concise notation should be self-explaining.

(I) Explicit computation of t and t^*:

1. Calculate current thickness: $t := t_0 \cdot \exp\left(-(\varepsilon_{1,\mathrm{top}} + \varepsilon_{2,\mathrm{top}})\right)$
2. Using Eq. (12): $\mathbf{FLC}_{\mathrm{mid}} := \mathrm{top2midplane}(\mathbf{FLC}_{\mathrm{top}}, t)$
3. Using Eq. (13): $\mathbf{FLC}_{\mathrm{bot}} := \mathrm{midplane2bottom}(\mathbf{FLC}_{\mathrm{mid}}, t)$
4. Calculate current thickness: $t^* := t_0^* \cdot \exp\left(-(\varepsilon_{1,\mathrm{bot}} + \varepsilon_{2,\mathrm{bot}})\right)$
5. Using Eq. (12): $\mathbf{FLC}^*_{\mathrm{mid}} := \mathrm{bottom2midplane}(\mathbf{FLC}_{\mathrm{bot}}, t^*)$
6. Using Eq. (13): $\mathbf{FLC}^*_{\mathrm{top}} := \mathrm{midplane2top}(\mathbf{FLC}^*_{\mathrm{mid}}, t^*)$

After the last step a new FLC is obtained, which is based on the original FLC pertaining to another thickness. As one may see, the last three steps reverse the first three ones, however using the new undeformed thickness t^* instead of t.

(II) Implicit computation of t and t^*:

1. Set start value for current thickness: $t := t_0$
2. Using Eq. (12): $\mathbf{FLC}_{\mathrm{mid}} := \mathrm{top2midplane}(\mathbf{FLC}_{\mathrm{top}}, t)$
3. Using Eq. (15): Calculate updated thickness: $t_{\mathrm{new}} := \frac{t_0}{(1+e_{1,\mathrm{mid}})\cdot(1+e_{2,\mathrm{mid}})}$
4. Continue if $|t_{\mathrm{new}} - t| < \mathrm{tolerance}$, else set $t := t_{\mathrm{new}}$ and go to step 2
5. Using Eq. (13): $\mathbf{FLC}_{\mathrm{bot}} := \mathrm{midplane2bottom}(\mathbf{FLC}_{\mathrm{mid}}, t)$
6. Set start value for current thickness: $t^* := t_0^*$
7. Using Eq. (12): $\mathbf{FLC}^*_{\mathrm{mid}} := \mathrm{bottom2midplane}(\mathbf{FLC}_{\mathrm{bot}}, t^*)$

8. Using Eq. (15): Calculate updated thickness: $t^*_{\text{new}} := \frac{t^*_0}{(1+e^*_{1,\text{mid}})\cdot(1+e^*_{2,\text{mid}})}$
9. Continue if $|t^*_{\text{new}} - t^*| < \text{tolerance}$, else set $t^* := t^*_{\text{new}}$ and go to step 7
10. Using Eq. (13): $\mathbf{FLC}^*_{\text{top}} := \text{midplane2top}(\mathbf{FLC}^*_{\text{mid}}, t^*)$

The iterations in the implicit scheme ensure that the correct current thickness is used.

As one may see, the implicit scheme is computationally more demanding than the explicit one. While the explicit scheme is convenient for direct calculations, it suffers from the fact that it causes an intrinsic error, as will be discussed below. This error can be avoided by using the implicit procedure, which is generally preferable.

Remark. Unless stated otherwise, the *implicit* strain calculation will be used throughout the present paper. □

In principle, the outlined explicit or implicit computation scheme can be used to calculate both the major and the minor strains pertaining to t^*_0. However, in the present work only the *major* strains are calculated in this way. The *minor* strains are computed using Eq. (18):

$$(\varepsilon^*_{2,\text{top}})_k = (\varepsilon_{2,\text{top}})_k \cdot \frac{(\varepsilon^*_{1,\text{top}})_k}{(\varepsilon_{1,\text{top}})_k} \tag{19}$$

Remark. Alternatively, the computation of the major and minor strains could have been done in the *reverse* order, i.e. calculate first $(\varepsilon^*_{2,\text{top}})_k$ using the algorithm above, followed by a calculation of $(\varepsilon^*_{1,\text{top}})_k$ using Eq. (18). Hence, the computation of the strain components is not unique. However, numerical tests revealed that the results of the alternative procedure are less realistic. □

Intrinsic Error of the Explicit Strain Calculation

In the *neutral case* $t_0 = t^*_0$ it can be expected that the previously described procedure just reproduces the input data, given that nothing has changed. However, this is not *exactly* the case when using the *explicit* method described above, because the explicit strain calculation of the current thicknesses t and t^* introduces a small error, as explained next. In case of bending, Eq. (2) yields

$$\left(e_{1,\text{top}} + e_{2,\text{top}}\right) > \left(e_{1,\text{mid}} + e_{2,\text{mid}}\right) > \left(e_{1,\text{bot}} + e_{2,\text{bot}}\right) \tag{20}$$

By means of the conversion

$$\varepsilon_j = \ln\left(1 + e_j\right) \tag{21}$$

the order in Eq. (20) is equivalent to

$$\left(\varepsilon_{1,\text{top}} + \varepsilon_{2,\text{top}}\right) > \left(\varepsilon_{1,\text{mid}} + \varepsilon_{2,\text{mid}}\right) > \left(\varepsilon_{1,\text{bot}} + \varepsilon_{2,\text{bot}}\right) \tag{22}$$

This, in turn, is equivalent to

$$\exp\left(-\left(\varepsilon_{1,\text{top}} + \varepsilon_{2,\text{top}}\right)\right) < \exp\left(-\left(\varepsilon_{1,\text{mid}} + \varepsilon_{2,\text{mid}}\right)\right) < \exp\left(-\left(\varepsilon_{1,\text{bot}} + \varepsilon_{2,\text{bot}}\right)\right) \tag{23}$$

Now, we consider the equation

$$t := t_0 \cdot \exp\left(-\left(\varepsilon_{1,\text{top}} + \varepsilon_{2,\text{top}}\right)\right) \tag{24}$$

to calculate the current material thickness t based on the *top* surface strains, as they are the sole explicitly available strain information. However, the thickness t calculated from Eq. (24) is only exact if *strain gradients* across the thickness of the sample associated with bending deformation were *absent*, which corresponds to $\varepsilon_{j,\text{top}} = \varepsilon_{j,\text{mid}} = \varepsilon_{j,\text{bot}}$. In fact, in the presence of strain gradients, Eq. (24) describes a kind of "local thickness" corresponding to the top surface and, as Eq. (23) reveals, a different thickness will be obtained if e.g. the (unfortunately unknown) midplane strains $\varepsilon_{j,\text{mid}}$ or bottom strains $\varepsilon_{j,\text{bot}}$ were used instead. Thus, using e.g. the top surface strains to calculate the "midplane thickness" will inevitably cause an error if strain gradients across the thickness are present.

The same error adheres to the equation

$$t^*: = t_0^* \cdot \exp\left(-\left(\varepsilon_{1,\mathrm{bot}} + \varepsilon_{2,\mathrm{bot}}\right)\right) \tag{25}$$

which, even worse, uses the previously *calculated* bottom strains, as they are the sole explicitly available strain information.

By virtue of Eq. (23) it is clear that the thicknesses t and t^*calculated by Eq. (24) and Eq. (25), respectively, are not objective, because they depend on the location of strain evaluation across the sample's thickness.

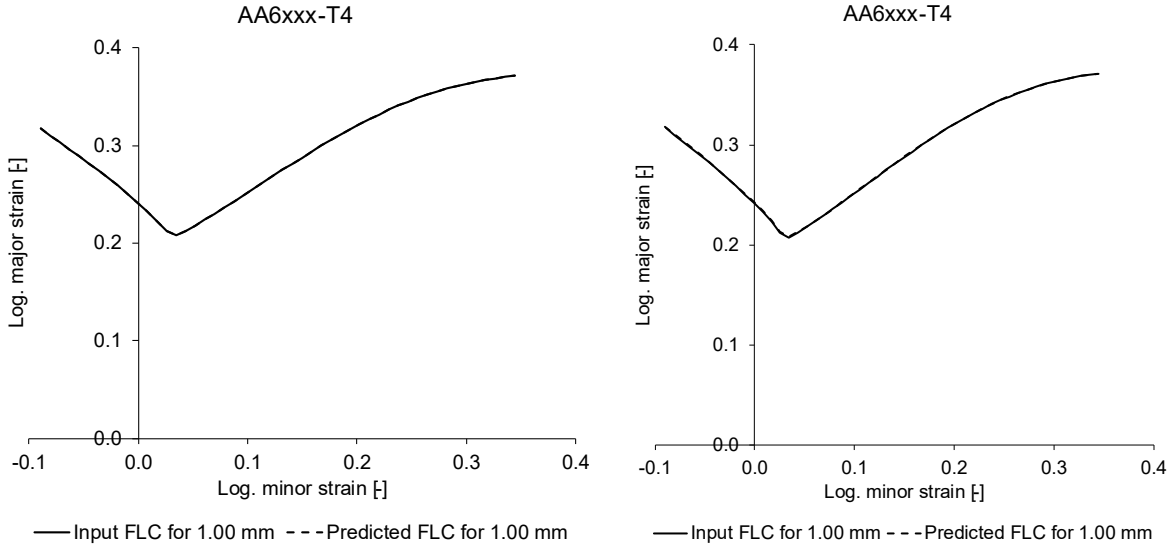

Fig. 1. Neutral case analysis for an AA6xxx-T4 material. Left: results of the implicit solution scheme. Right: results of the explicit solution scheme.

From the explanations just given, one may conclude that the same error is made *twice* in the explicit computations, which is the reason why inaccuracies must be expected. Since the strain gradients caused by bending increase with t_0, one may expect that the error will grow accordingly when using the explicit method. Numerical experiments of the author (not shown) confirm that the intrinsic error of the explicit strain calculation positively correlates with t_0.

As an example, consider the results in Fig. 1 of two neutral case predictions for a 6xxx aluminium alloy for $t_0 = t_0^* = 1$ mm using both the implicit and the explicit solution scheme. As one may see, in either case the input curve and the prediction are virtually identical, revealing a negligible error of the explicit scheme. However, another application example considered below demonstrates that the intrinsic error cannot be neglected in general.

Application Example: 5xxx Aluminium Alloy

The considered material is an AA5182 aluminium alloy in H2x temper with a gauge of $t_0 = 3$ mm. The FLC data shown in Fig. 2 (left) were acquired according to the standard DIN EN ISO 12004-2 using a punch radius of $R_\mathrm{p} = 50$ mm and with 3 repetitions for each sample geometry (throughout all FLCs in this paper). The experimental data points were fitted using a third-order polynomial.

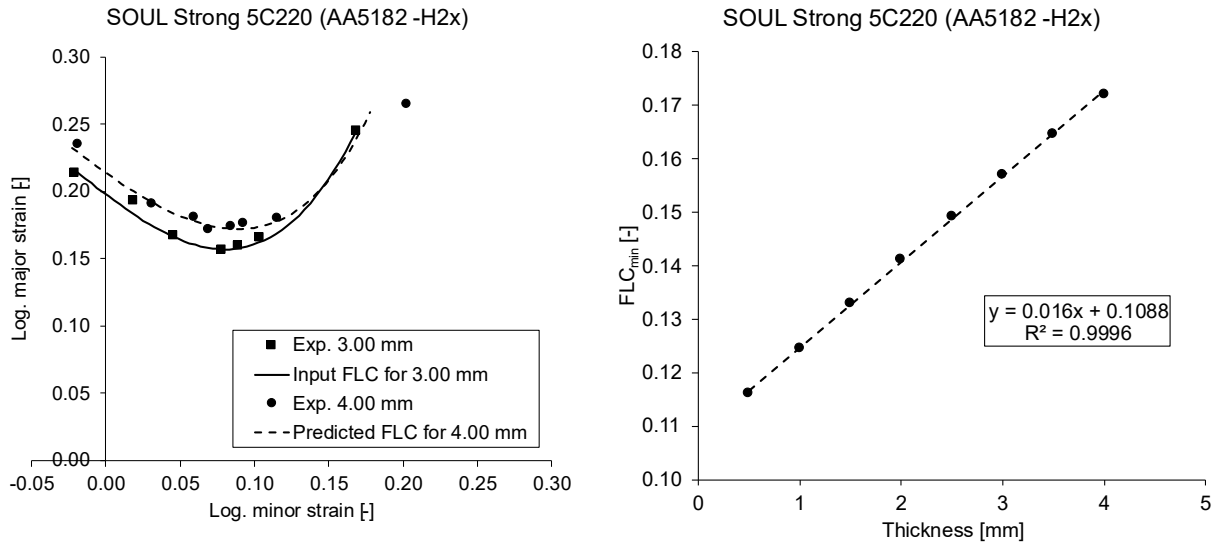

Fig. 2. FLC data and prediction pertaining to the AA5182-H2x material.

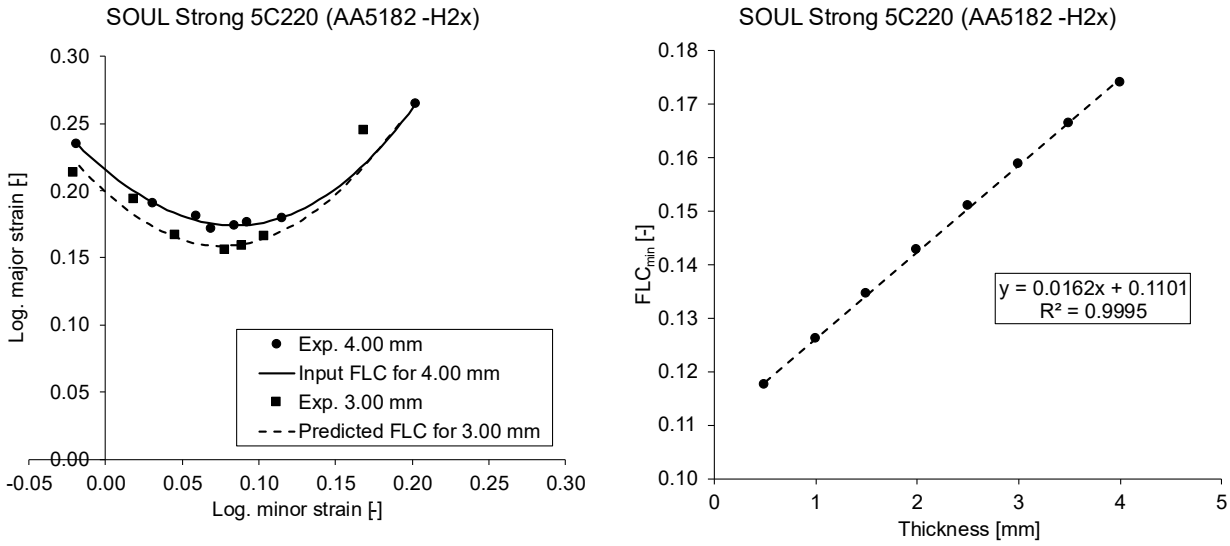

Fig. 3. FLC data and prediction pertaining to the AA5182-H2x material (reverse analysis).

The developed thickness scaling method was used to make a *blind* prediction of the FLC pertaining to a larger thickness of $t_0^* = 4$ mm. The necessity for a blind prediction arose from a customer request since at its time no experimental data pertaining to $t_0^* = 4$ mm were available. Later, the material with a gauge of $t_0^* = 4$ mm was produced, which enabled its FLC determination. As Fig. 2 (left) reveals, in the present case the blind prediction matches the experimental FLC very well.

It is also very interesting to use the developed theory to predict the major strain pertaining to the minimum point of the FLC, commonly denoted as $\mathrm{FLC_{min}}$, for different gauges. As Fig. 2 (right) reveals, a linear relationship is obtained which is, qualitatively, in agreement with experimental findings.

Remark. The $\mathrm{FLC_{min}}$-predictions in Fig. 2 (right) are based on the reference FLC pertaining to a gauge of $t_0 = 3$ mm. Consequently, if this reference FLC changes slightly, e.g. due to batch variations, then the $\mathrm{FLC_{min}}$-predictions will be affected accordingly. □

Next, a *reverse analysis* is carried out: we now pretend that solely the FLC pertaining to $t_0 = 4$ mm was given and wish to predict the FLC pertaining to $t_0^* = 3$ mm. Since experimental FLC data are available for both gauges it is straightforward to quantify the prediction. The results of this analysis are summarized in Fig. 3 (left) and reveal a very good prediction of the target FLC. It is also

interesting to investigate whether the reverse analysis results in a different $\mathrm{FLC}_{\mathrm{min}}$-prediction, which is shown in Fig. 3 (right): a direct comparison with Fig. 2 (right) reveals rather minor differences.

The available data may also be used to investigate the *intrinsic error* related to the *explicit* solution scheme as discussed above. To this end, the *neutral case* $t_0 = t_0^* = 4$ mm is considered. This rather large gauge is very well suited for an error analysis, because the intrinsic error, as discussed above, positively correlates with thickness. The corresponding results in Fig. 4 (right) reveal a small overprediction compared to the input curve. A simple way to roughly quantify this error is to evaluate the $\mathrm{FLC}_{\mathrm{min}}$-values, which are $\mathrm{FLC}_{\mathrm{min}} = 0.174$ and $\mathrm{FLC}^*_{\mathrm{min}} = 0.182$, respectively, corresponding to an overprediction of ≈ 4.6 %. To demonstrate its superiority over its explicit equivalent, the neutral case analysis was also carried out using the *implicit* strain calculation, see Fig. 4 (left), in which case the input and the predicted FLC coincide.

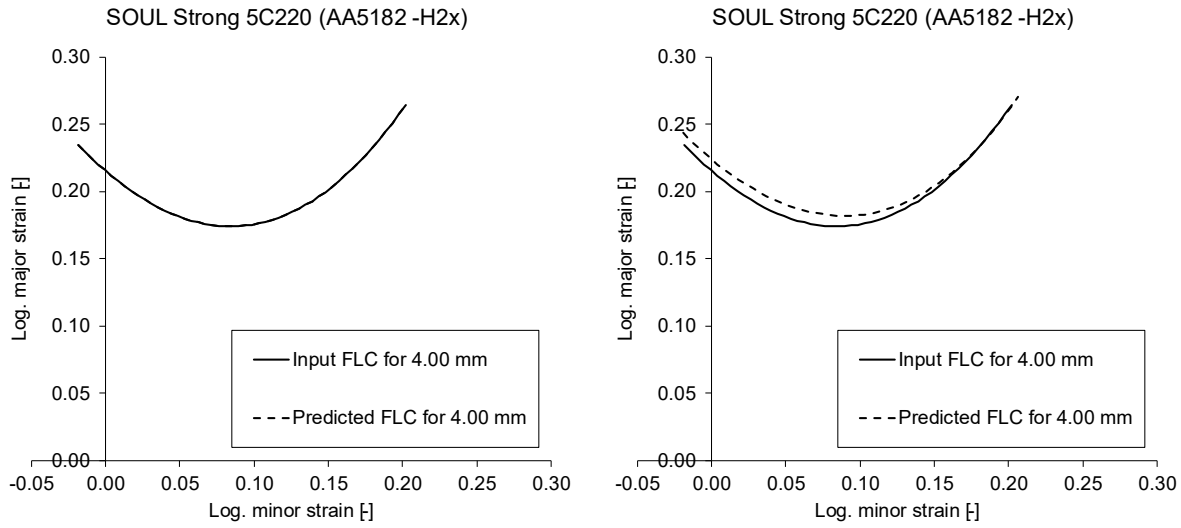

Fig. 4. Neutral case analysis for the AA5182-H2x material. Left: results of the implicit solution scheme. Right: results of the explicit solution scheme.

Remark. As explained above, the proposed method can only account for *kinematic* effects related to bending deformation. Thus, *microstructural* effects, such as those observed by Suh *et al.* [6], are not considered *per se*. However, a respective extension of the kinematic method appears feasible. For example, an *ad hoc* approach could be to carry out uniaxial tensile tests for two different gauges, and to add the *engineering* fracture strain difference to the *engineering* major strain of the scaled FLC *a posteriori*. (Note that when extensometers are used *true* fracture strains cannot be determined in a theoretically consistent way.) Of course, this presumes that fracture strains are already available for both gauges. If this is not the case, one may think of interpolating available data pertaining to other gauges. For the AA5182-H2x material considered in the present work, this extra contribution amounts to an engineering strain of $+0.007$ when the sample thickness *increases* from 3 mm to 4 mm, and would only slightly *increase* the major strain of the scaled FLC. (Note that when the sample thickness *decreases*, the extra strain contribution would be *negative*, thereby *decreasing* the major strain of the scaled FLC.) One may speculate that the *absolute* value of this extra strain contribution increases when the thickness contrast is larger than in the case considered. However, a detailed investigation is beyond the scope of the present work and left for future research. □

Summary

A consistent kinematic method was developed to calculate a forming limit curve (FLC) for a material thickness t_0^* from a given FLC pertaining to a different thickness t_0. The developed method is based on the analysis of the bending strains introduced by the Nakajima test method. The calculation procedure may be broken down in two major steps: in the first step, the top surface strains of the

given forming limit curve are used to calculate the corresponding bottom surface strains; in the second step, the calculated bottom surface strains are used to calculate the top surface strains using the desired new material thickness. To calculate the required strains, an explicit and an implicit procedure were presented. In contrast to its implicit equivalent, the explicit method suffers from an intrinsic error which scales with the material's gauge and can be quantified by considering the neutral case $t_0^* = t_0$. For a rather large thickness, an application example illustrates that the intrinsic error of the explicit strain calculation causes an overprediction of $\mathrm{FLC}_{\mathrm{min}}$ of about 4.6 %. Finally, the developed method predicts a linear relationship between $\mathrm{FLC}_{\mathrm{min}}$ and the material thickness, which is in line with practical experience. The proposed method does not account for microstructural features potentially contributing to the scaled FLC. A respective *ad hoc* extension of the kinematic method was outlined but not investigated in detail.

Acknowledgements

The author is grateful to Dr. Henk-Jan Brinkman for stimulating this work.

References

[1] M. Abspoel, M. E. Scholting, J. M. M. Droog, A new method for predicting Forming Limit Curves from mechanical properties, Journal of Materials Processing Technology 213 (2013) 759-769.

[2] H. Aretz, Pre-strain correction of forming limit curves, Materials Research Proceedings 41 (2024) 948-957.

[3] E. Axelrad, Schalentheorie, B. G. Teubner Stuttgart, 1983.

[4] D. Banabic, H.-J. Bunge, K. Pöhlandt, A. E. Tekkaya, Formability of Metallic Materials, Springer-Verlag Berlin Heidelberg GmbH, 2000.

[5] J. Noder, C. Butcher, A comparative investigation into the influence of the constitutive model on the prediction of in-plane formability for Nakajima and Marciniak tests, International Journal of Mechanical Sciences 163 (2019) 105138.

[6] C. H. Suh, Y.-C. Jung, Y. S. Kim, Effects of thickness and surface roughness on mechanical properties of aluminum sheets, Journal of Mechanical Science and Technology 24 (2010) 2091-2098.

[7] S. Timoshenko, J. M. Gere, Theory of Elastic Stability, 2nd ed., Dover Publication, 2009.